Study on Composite Material for Shielding Mixed Neutron and γ-Rays

Huasi Hu, Qunshu Wang, Juan Qin, Yuelei Wu, Tiankui Zhang, Zhongsheng Xie, Xinbiao Jiang, Guoguang Zhang, Hu Xu, Xiangyang Zheng, Jing Zhang, Wenhao Liu, Zhenghong Li, Boping Zhang, Linbo Li, Zhaohui Song, Xiaoping Ouyang, Jun Zhu, Yaolin Zhao, Xiaoqin Mi, Zhengping Dong, Cheng Li, Zhenyu Jiang, and Yuanping Zhan

***Abstract*—Optimized lightweight, compact and high temperature sustaining shielding materials for neutron and gamma radiation were developed by genetic algorithms (GA) combined with the Monte Carlo N-Particle (MCNP) code. A series of samples were designed according to the method. Deep penetration tests by the MCNP code were completed. The results show that the designed samples have more advantages related to the radiation shielding effects in comparison with PB202 and KRAFTON-XP3, especially the Cakes with multi-layers structures of the Fe-Interlayer-Pb have excellent performance. Taking into account the ratios designed of components among elements in the material, the manufacturing process of polymer with nano-TiO_2 was studied experimentally by differential scanning calorimetry (DSC). Several samples have been tested. The attenuation experiments on the samples were carried out using tandem electrostatic accelerator neutron source, spontaneous fission neutron source of ^{252}Cf and γ-rays source of ^{60}Co. The experimental results verify the correctness of optimal design and craft. The Cakes are quite suitable for applications in the practices of nuclear science and technology.**

***Index Terms*—Composite, gamma rays, genetic algorithms, Monte Carlo, neutrons, shielding.**

Manuscript received November 20, 2007; revised February 22, 2008. Current version published September 19, 2008. This work was supported by the National Natural Science Foundation of China (10576022) and NINT Contract 200509006.

H. Hu, J. Qin, Y. Wu, T. Zhang, Z. Xie, B. Zhang, J. Zhu, Y. Zhao, C. Li, Z. Jiang, and Y. Zhan are with the School of Nuclear Science and Technology, Xi'an Jiaotong University (XJTU), Xi'an, 710049 Shannxi, China (e-mail: huasi_hu@mail.xjtu.edu.cn; pearl1017@stu.xjtu.edu.cn; wuyuelei@stu.xjtu.edu.cn; china-ztk@stu.xjtu.edu.cn; zsxie@mail.xjtu.edu.cn; boping.zhang@stu.xjtu.edu.cn; chujun@xjtu.edu.cn; zhaoyaolin@mail.xjtu.edu.cn).

Q. Wang, X. Jiang, and Z. Song are with the Nor-west Institute of Nuclear Technology (NINT), Xi'an, 710024 Shaanxi, China (e-mail: wqs02@mails.thu.edu.cn; jiangxb67@yahoo.com.cn; szh197107@126.com).

G. Zhang is with the Nor-west Institute of Nuclear Technology (NINT), Xi'an, 710024, Shaanxi, China and also with the China Institute of Atomic Energy (CIAE), Beijing 102413, China (e-mail: kogunchiang@gmail.com).

H. Xu is with the School of Nuclear Science and Technology, Xi'an Jiaotong University (XJTU), Xi'an, 710049 Shannxi, China. and also with the Wuhan Secondary Institute of Ships, Wuhan, 430064 Hubei, China (e-mail: xhu_xu@hotmail.com).

X. Zheng is with the School of Nuclear Science and Technology, Xi'an Jiaotong University (XJTU) Xi'an, 710049 Shannxi, China and also with the Nuclear and Radiation Safety Centre, State Environmental Protection Administration (SEPA) Beijing 100082, China (e-mail: mana@stu.xjtu.edu.cn).

J. Zhang and W. Liu are with the School of Nuclear Science andTechnology, Xi'an Jiaotong University (XJTU), Xi'an, 710049 Shannxi, China and also with the China Guangdong Nuclear Power Holding Co. Ltd., Shenzhen, 518124 Guangdong, China (e-mail: nuclearjing@163.com; hncslwh@sina.com).

Z. Li and L. Li are with the Institute of Nuclear Physics and Chemistry, CAEP, Mianyang, 621900 Sichuan, China (e-mail: lee66918@yahoo.com; heroboer@sina.com).

X. Ouyang is with the School of Nuclear Science and Technology, Xi'an Jiaotong University (XJTU) Xi'an, 710049 Shannxi, China and also with the Nor-west Institute of Nuclear Technology (NINT), Xi'an, 710024 Shaanxi, China (e-mail: oyxp2003@yahoo.com.cn).

X. Mi and Z. Dong are with the School of Nuclear Science and Technology, Xi'an Jiaotong University (XJTU) Xi'an, 710049 Shannxi, China and also with the Nuclear Power Institute of China, Chengdu, 610041 Sichuan, China (e-mail: mixiaoqin@126.com).

Color versions of one or more of the figures in this paper are available online at http://ieeexplore.ieee.org.

Digital Object Identifier 10.1109/TNS.2008.2000800

I. Introduction

NUCLEAR radiation shielding material is an important infrastructure component in nuclear facilities [1]–[3] such as nuclear reactors and particle accelerators. Especially in mobile nuclear devices and manned spacecrafts [4], [5], owing to the limits of space and maneuverability, the weight and volume of radiation shielding material are restricted. Thus radiation shielding materials must have high effective shielding properties. Usually shielding materials have to service for a long time in quite inclement environment with high temperature, corrosion, and so on. Furthermore, shielding materials could be damaged by constant radiation due to interaction with each other [6], [7]. Therefore radiation shielding materials must have multiple endurances in many environments including radiation effects, heat, etc. Certainly, the cost of material is also an important requirement to be considered in the project. And then efforts must be made to reduce the exposure of employees in nuclear facilities on basis of the as-low-as-reasonably-achievable (ALARA) principle [8].

The polyethylene and polyethylene mixed with boron oxide are widely used as neutron shielding materials, but they have poor mechanical strength, poor thermal stability and poor durability for neutron and gamma irradiation; they can not be in service for a long time [9], [10].

The most effective shielding material for nuclear reactors is obtained by mixed hydrogenous materials, heavy metal elements, and other neutron absorbers. Inelastic scattering by heavy elements and elastic scattering by hydrogen are quite effective to slow down fast and intermediate energy neutrons, and the absorbers can reduce secondary gamma rays as well as thermal neutrons. Then the hydrogenous epoxy resin with excellent radiation resistant ability and high thermal stability should be selected as the substrate of the composite material with some reinforced particles such as Fe, Pb, W, B_4C and Gd_2O_3 powder. In addition, a small quantity of nano-TiO_2 powder could be applied to enhance the thermal stability and toughness of the composite material [11]–[13].

The method of fission neutrons removal cross sections to calculate radiation shielding can be found in some references [14]–[16]. But there are two problems that have not been solved thoroughly: attenuation of low energy neutrons (including thermal and epithermal groups) and inelastic scattering of fast neutrons (fast group). Therefore, a new method to design the optimized shielding material for fission neutrons and γ-rays mixed radiation fields is proposed by using Genetic Algorithms (GA) [17] with the MCNP code [18]. This way some new material can be designed.

Epoxy resin is made by mixing a main agent with the curing agent. Generally the main agent could be chosen from many kinds of resins such as epoxy, polyimide and bismaleimide (BMI). In spite of the best heat resistance of BMI, bisphenol A should be selected because of its high content of hydrogen elements for intermediate energy neutrons moderation. In this project, the E-51 bisphenol A, a waterborne epoxy resin was chosen. The curing agent could be chosen from multi-amine and anhydride. The multi-amine mainly refers to polyamide because of the low cost and the widespread use. The practical way of making anhydride is usually to mix varieties of anhydride to substantially improve the thermal deformation temperature of compounds.

However, it becomes difficult to cure when epoxy is mixed with foreign materials. Advanced technology that controls the curing heat and post-life (the time from mixing to curing) is required when making thick epoxy resin for shielding materials. Moreover, mixing with foreign materials reduces mechanical strength because mixing foreign materials is equal to resin loss. Some metal powders with good thermal conductivity could improve the heat resistance of compounds. The best mixing parameter thus has to be studied. Modification of the epoxy resins by nano-$\mathrm{TiO_2}$ can be studied systematically through thermal analysis techniques. Then the forming process craft of the new composite material can be obtained and a series of radiation shielding composite material samples is made.

The attenuation experiments were carried out to check neutron and γ-rays shielding performance of the new shielding material by using tandem electrostatic accelerator neutron source, spontaneous fission neutron source of $^{252}\mathrm{Cf}$ and γ-rays source of $^{60}\mathrm{Co}$. The samples of new composites have been tested. Meanwhile, correctness of optimal design method and trial-manufacture craft of shielding material has been also verified.

II. Development of the New Type of Shielding Material

A. GA Application in Designing Shielding Material

For the optimal design of shielding material, the dose equivalent corresponding to 2.407 neutrons and 7.77 γ photons (these are the average number released per fission event [19], [20]) with fission energy spectra in one fission process penetrating a specific thickness of the shielding material was selected applying the optimized objective function [21]

$$\min f(X) = [f_n(X), f_g(X)]^T \tag{1}$$

that subjects to the constraints: equalities, inequalities and domain constraints. They depend on the uniformity of the composite material components, the component range of every element in composite from minimum to maximum, and the density of composite materials:

$$\sum_{i=1}^{N} x_i = 1 \tag{2}$$

$$L \le X \le U \tag{3}$$

$$\rho(X) \in D \tag{4}$$

$$\frac{1}{\rho(X)} = \sum_{i=1}^{n} \frac{1}{\rho_i} x_i. \tag{5}$$

Where,

N	the number of components in composite material
$X = (x_1, x_2, \ldots x_N)$	the variable vector, mass components matrix in composite material
$f(X)$	total dose equivalent of neutrons and γ-rays with fission energy spectra in one time fission process penetrating a specific thickness of the shielding material, Sv
$f_n(X)$	dose equivalent of fission neutron, Sv
$f_g(X)$	dose equivalent of fission γ-rays, Sv
L, U	components vectors of minimum & maximum respectively
$\rho_i, \rho(X)$	density of single component and composite material, $g \cdot \mathrm{cm}^{-3}$
D	vector of the density ranges.

There are four steps in the GA optimization design program shown in Fig. 1. Firstly, the raw materials are selected from the present materials (simple elements or compound materials) in the world. In the process of selecting, the cost and the radiation shielding capability are mainly concerned. Their physical and chemical capability, mechanical and thermal properties are also considered. Secondly, according to a component material ratio assumed originally, each materials density, and all other parameters were edited in the proper MCNP input files: "inpn" and "inpp". After that, MCNP calculates one fission neutron dose equivalent Hn (in output file outpn), one fission γ photon dose equivalent Hp (in outpp), and the total dose equivalent $\mathrm{H}(= 2.407\mathrm{Hn} + 7.77\mathrm{Hp})$ of the neutrons and γ-rays per fission. Thirdly, the GA program can transfer the MCNP results at every generation in every count, if so needed. Finally, the object function for optimizing design is a certain function, based on constraint conditions confirmed by some calculations.

TABLE I
SHIELDING MATERIAL ELEMENT CONTENTS OPTIMAL DESIGNED /w%

element	H	^{10}B	^{11}B	C	O	Ti	Fe	Gd	W	Pb	density/ $g \cdot cm^{-3}$
Jxa1	2.266	0.136	0.581	17.88	5.307	0.06	0	1.736	5.013	67.29	3.38
Jxa2	2.45	0.078	0.31	18.5	5.31	0.06	0	1.74	12.67	57.73	3.53
Pb6	1.523	0.366	1.466	14.567	5.056	0.379	0	0	14.436	62.186	3.72
Djy	0	0	0	26.28	1.95	0	50.17	12.80	8.80	0	5.7
Interlayer	8.19	0.16	0.64	65.87	18.43	0.93	0	5.78	0	0	1.48

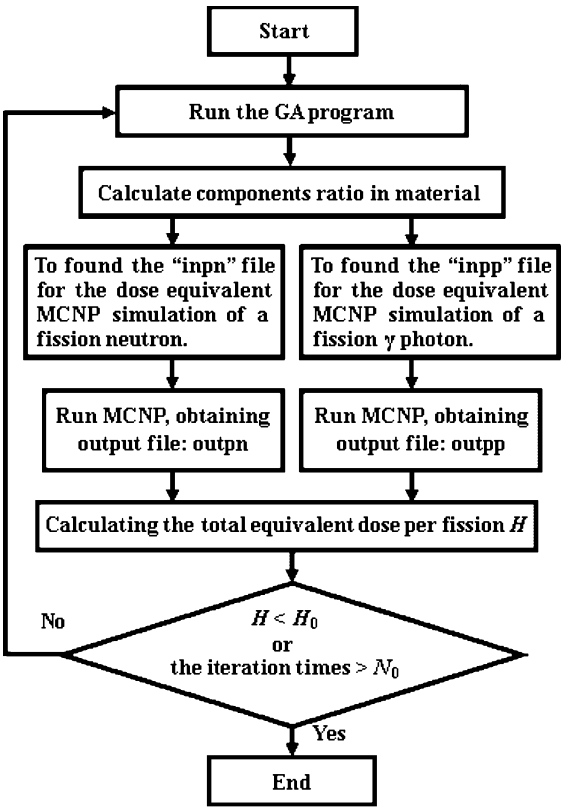

Fig. 1. Flow chart of material optimal design with GA and MCNP code.

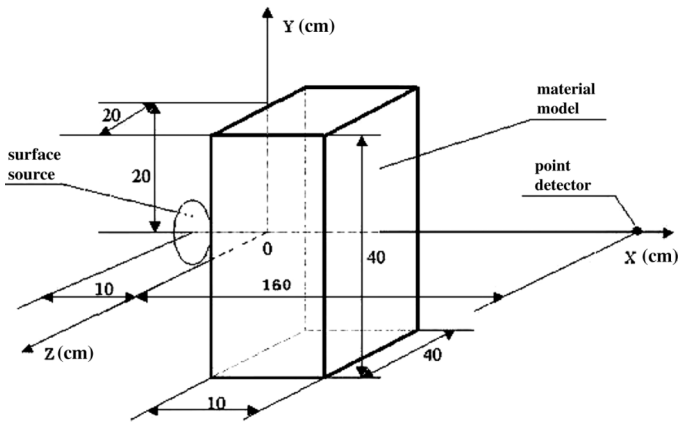

Fig. 2. MCNP simulation model.

The cumulative probability distribution q is selected between 0.15–0.35 according to population size, and higher q values provide stronger selective pressure [17].

MCNP simulation model (INP files) for neutrons or γ-rays emitted from a surface source penetrating a slab material is shown in Fig. 2. Point flux detectors were used. As to fission neutron, Watt energy spectrum and "mode n p" were used, secondary gamma rays were also be counted. As to fission gamma rays, "mode p" was used. A prompt γ-rays spectrum distribution empirical formula was employed [20]:

$$N(E_\gamma) = \begin{cases} 6.6\gamma - rays/fission - \text{MeV} & 0.1 < E_\gamma \le 0.6\,\text{MeV} \\ 20.2\exp(-1.78E_\gamma) & 0.6 < E_\gamma \le 1.5\,\text{MeV} \\ 7.2\exp(-1.09E_\gamma) & 1.5 < E_\gamma \le 10.5\,\text{MeV}. \end{cases} \quad (6)$$

By running the optimal design program, a series of materials optimized ratios have been obtained. They are listed in Table I. Jxa1 and Jxa2 are polyamide composites, Pb6 is anhydride composite, Djy is another composite suited to powder forming with heat isostatic pressing (HIP). Interlayer is also polyamide composite without Fe, W and Pb.

TABLE II
THE PROCESSED MATERIALS USING IN EXPERIMENTS

Components/g	Samples1/2/3/4/5/6/7
bisphenol A(E_51)	100
PMDA	21
MA	19
epoxy propane butylether	10
Pb	525
Fe	75
nana-TiO_2(rutile)	1/2/3/4/5/10/30
Total mass/g	751/752/753/754/755/760/780

B. Experimental Research on Manufacturing Process

As an example, the manufacturing process experiment of composite mixing bisphenol A with the mixed curing agent is introduced below. The experimental samples consist of the following components: E-51 bisphenol A, waterborne epoxy resin, the mixed curing agent pyromellitic dianhydride (PMDA), maleic anhydride (MA), the active diluents (epoxy propane butyl ether), the reinforced material powder (nano-TiO_2), Fe and Pb powder. In the molding-craft of the polymer, the solidifying process is most important. Table II lists seven kinds of experimental samples with nano-TiO_2 in different mass contents.

The solidifying temperature and time directly affects the performances of the composite solidified-form, thus the optimization of the solidifying process is extremely necessary. Especially PMDA and MA are selected as curing agent while foreign materials (Pb, Fe, etc) are mixed, it is difficult to confirm the changes during the solidifying process accurately. This paper establishes the unstable temperature field and solidifying

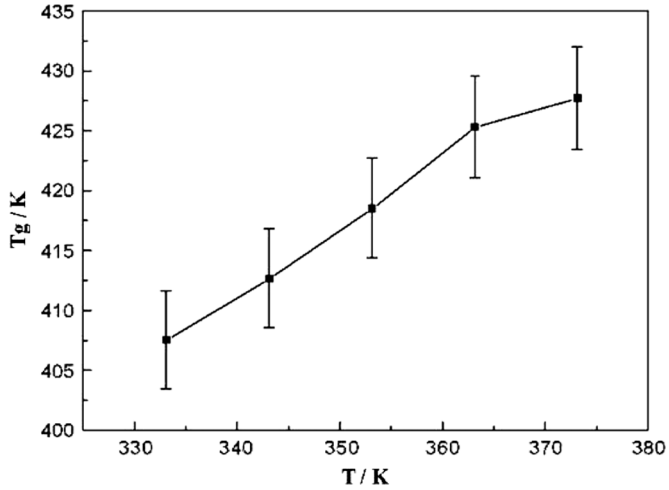

Fig. 3. Tg versus the temperature of isothermally curing of sample 3.

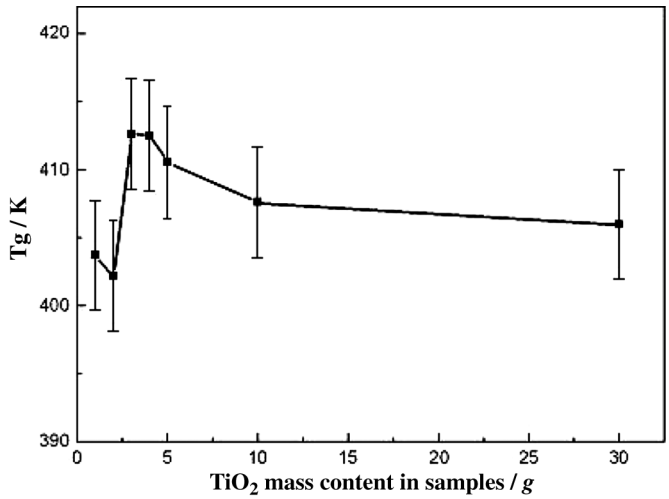

Fig. 4. Tg versus the mass content of the nano-TiO_2 in samples at 343 K.

reaction kinetics model. By using the differential scanning calorimetry (DSC) of the non-isothermally and isothermally solidifying, the parameters of solidifying kinetics and the solidified-form parameters in the model, such as the glassing temperature, solidifying time and so on have been analyzed and confirmed. The Q1000 V9.0 Build 275 DSC made in TA Co. Ltd. of USA (New Castle, Delaware) was employed in experiments.

Nano-TiO_2 enhances the toughness and increases the thermal deformation temperature. Besides, it can reduce the solidification temperature of epoxy resin. Two experiments were performed under two different conditions. The first using the same mixture ratio but varying temperatures is shown in Fig. 3. The second using various mixture ratios and the same temperature is shown in Fig. 4. At last the optimizing mixture ratio and solidification temperature are confirmed. It shows that nano-TiO_2 with the mass content about 3g in samples can enhance the glass transition temperature (Tg) of the epoxy resin about 10K, and reduce solidification temperature about 10K. That proves that nano-TiO_2 only reacts on the epoxy resin because they were fully emulsified.

III. Deep Penetration Tests by the MCNP Code

The composite material samples designed in Table I have been made according to the trial-manufacture craft. The radiation shielding performance of the materials in deep penetration can be tested by MCNP code. Fig. 5 shows the shielding effects to neutrons and γ-rays per fission event. Multi-layers ($Fe/CH_2/Pb = 6/3/1$, thickness ratio) is on service at some nuclear applications now. The lead-borated polyethylene was successively developed by the Reactor Experiments Inc. of American (R/X material # 202) [22] and the Nuclear Power Institute of China (PB202) [23]. The KRAFTON-XP3 was developed by Sanoya Industry Co. Ltd. of Japan [24]. The Cakes (Cake1 only in Fig. 5) and Djy have excellent shielding performances:fission neutron [Fig. 5(a)] and γ-rays (b) shielding effects are the best of composites, inhibition effects of secondary γ-rays of fission neutron (c) are also very good, comprehensive shielding effect of fission neutrons and γ-rays is the most prominent (d). The remaining shielding materials optimal designed (Jxa1, Jxa2 and Pb6) have also good performance. Table III lists the Fe-Interlayer-Pb thickness ratios of Cakes.

The thickness ratio of Cakes was optimized and listed in Table III. The first layer iron is quite effective to slow down the fast neutrons to intermediate neutrons by inelastic scattering. The middle layer is the Interlayer which not only slows down intermediate neutrons to thermal neutrons by elastic scattering on hydrogen (8.19w%) effectively, but also captures thermal and intermediate neutrons by boron-10 (0.16w%) and gadolinium (5.16w%). The last layer, lead, can attenuate the γ-rays and the secondary γ-rays of neutrons. Iron and lead are the common shielding materials because of theirs low price and easy machining. But they cannot be used extensively due to the weight and volume limit. Therefore their thickness component ratio is optimized. The Cakes shielding capabilities were simulated. MCNP code was edited to calculate the shielding effects of various materials for fission neutrons gamma spectrum of ^{235}U. The results are shown in Fig. 5. Cake1 with equivalent density of $4.55g \cdot cm^{-3}$ has the best shielding performance.

Fig. 6 shows the changes of energy spectrum for fission neutron penetrating different thickness of Cake1 and PB202 simulated by MCNP. The results indicate that Cake1 is quicker to slow down the fast neutron than PB202. With thickness from 5 cm to 50 cm increasing the advantage has become more obvious.

Table IV lists several common used shielding material performances which relate to total shielding effect such as density, equivalent shielding thickness, thermal stability and radiation resistance. According to Table IV, the materials (in shading columns) optimized by GA combined with the MCNP code have excellent overall performance, especially Cakes have the most advantages in radiation shielding, heat resistance and radiation resistance. Though the Djy is also excellent, but its forming craft is very complicated and a large amount of products are difficulty to be obtained.

The radiation resistance of materials is a lumped indicator using to evaluate a variety of material parameters in irradiation environment. The materials parameters contain various content, such as mechanical, thermal, chemical and radiation chemical.

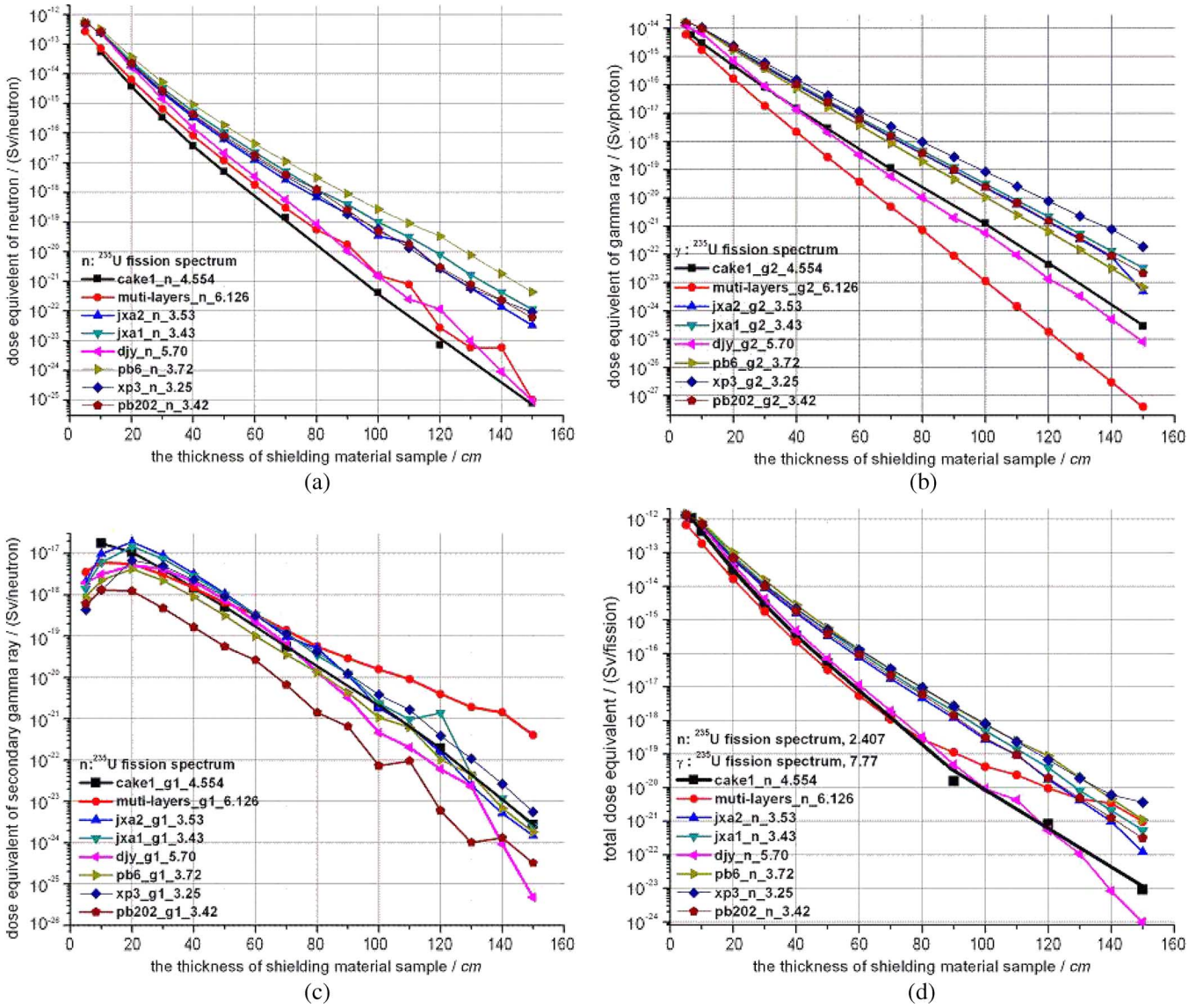

Fig. 5. Comparison among shielding materials by MCNP simulation to a fissile source. (a) One fission neutron; (b) one fission γ photon; (c) secondary γ-rays of one fission neutron; (d) total of neutrons and γ-rays in a fissile source.

TABLE III
Fe-INTERLAYER-Pb THICKNESS RATIOS OF CAKES

shielding material	Fe:Interlayer:Pb (thickness ratio)	equivalent density $/g \cdot cm^{-3}$
Cake 1	2.5:6:1.5	4.55
Cake 2	1.5:7:1.5	4.01
Cake 3	2:7:1	3.84

In addition, because the shielding materials generally contain polymer and inorganic (metal and nonmetallic) powders, the radiation resistance quantitative evaluation is very difficult. Certainly, the sub-indicators can be expected to achieve quantitative evaluation. In Table IV, we just list qualitative evaluation but not quantitatively evaluation. In quantitative comparison of the materials radiation resistance, epoxy resin is an excellent, polyethylene is much worse than epoxy resin, polyamide is even worse [25]–[27]. Therefore, when the material mixed with a large number of polyethylenes, its radiation resistance is evaluated as "lacking". If the material is made of epoxy resin mixed with a small amount of polyamide, its performance has reduced relative to epoxy resin and is evaluated as "good". Epoxy resins cured with the anhydrides, especially the aromatic types such as PMDA, display high-thermal stabilities, high heat distortion temperatures, high radiation resistance, etc [28]. Then if the material made of epoxy resin mixed with a small amount of anhydride is evaluated as "best". The incorporation of nano-TiO_2 particles into the epoxy resin improves the mechanical and thermal properties, and hardly improves the radiation shielding performance, but may indirectly enhance the radiation resistance. This needs to be further confirmed by experiment. Djy is similar to ceramic product and is also evaluated as "best". These evaluations are consistent with the summary by Schönbacher and Tavlet appears in CERN-94-07 [29].

TABLE IV
PERFORMANCES COMPARISON AMONG SHIELDING MATERIALS

shielding material	density $/g \cdot cm^{-3}$	thickness of attenuation one hundredth of the total dose equivalent/cm	heat-resistance $/^{\circ}C$	radiation resistance
PB202	3.42	21.5	<100	Lacking(containing about 19w% polyethylene)
KRAFTON-XP3	3.25	21.7	<150	good(small amount of curing agent:ployamine)
Iron(Fe)	7.86	38.5	1300	
Lead(Pb)	11.34	30.9	327	
Concrete1	2.51	33.3		
Concrete2	3.50	25.9		
Multi-layers	6.128	19.9	<100	lacking(containing polyethylene shield)
Diy	5.7	21.1	about 700	best(similar to ceramic)
Jxa1	3.38	23.6	about 200	good(small amount of curing agent:polyamine)
Jxa2	3.53	22.5	about 200	good(Ibid)
Pb6	3.72	25.0	>200	best(mixed curing agent:PMDA+MA)
Cake 1	4.55	16.4	about 200	good(in Interlayer,low content polyamine)
Cake 2	4.01	16.6	about 200	good(Ibid)
Cake 3	3.84	16.5	about 200	good(Ibid)

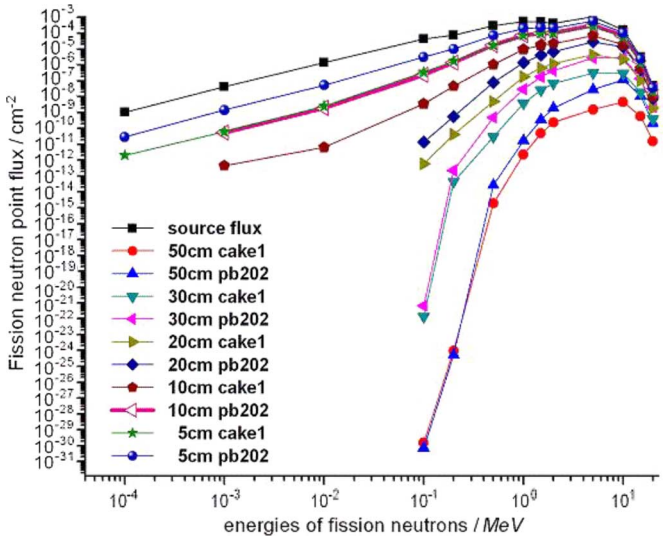

Fig. 6. Comparison on changes of energy spectrum for fission neutron penetrating different thickness of Cake1 and PB202 simulated by MCNP.

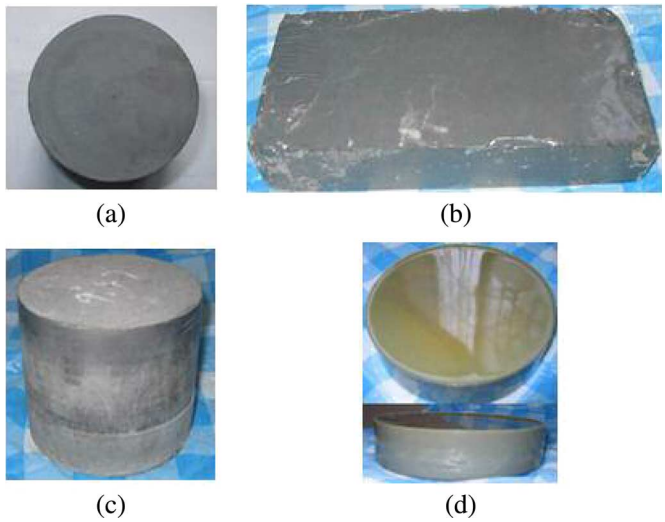

Fig. 7. Samples trial produced in project. (a) Jxa1. (b) Jxa2. (c) Pb6. (d) Interlayer.

IV. TRIAL PRODUCTION OF SAMPLES

According to the optimal designed element contents of shielding material listed in Table I and the manufacturing process, five kinds of composite shielding materials samples were trial-produced with 4 of these shown in Fig. 7. These samples were prepared for checking neutron and γ-rays shielding performance and testing the correctness of optimal design method and trial-manufacture craft of shielding material. The Djy samples were formed with hydraulic forming method and not shown here.

V. THE RESULTS OF GAMMA AND NEUTRON EXPERIMENTS

A. Gamma Attenuation Shielding Experiment

The experimental setup, shown in Fig. 8, consists of γ-rays source of ^{60}Co, collimator and NaI(Tl) γ-rays spectrometer. The total counts are the total measurement including background, and net counts are the measurement except background. X is the thickness of test material slab. When there is no shielding and X equals to zero, the detector net counts is

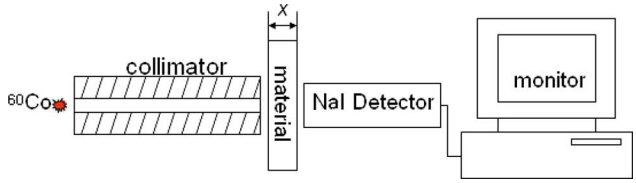

Fig. 8. The experimental setup diagram of γ-rays attenuation.

"1". The other measurements are relative to that. Because of measurement cost, only Cake1 and Multilayer samples were selected and the measurement results are listed in Table V.

In order to check the experimental results, the corresponding MCNP simulations were done. All the results are shown in Fig. 9. Cake1 experimental data and simulation data are in accord until 10 cm thickness. While the thickness of samples is bigger than 10 cm, before reaching the attenuation one hundredth of the gamma rays, the experimental data gradually downwards depart from the simulation data. When the dose buildup effect in experiment is revised quantitatively, the corrected data (dashed line in Fig. 9) back to the e exponential

TABLE V
γ-RAYS OF ^{60}Co ATTENUATION MEASUREMENT RESULTS IN TWO MATERIAL SAMPLES

shield & Density /$g \cdot cm^{-3}$	Thickness /cm	Counts Total	Counts Net area	Relative attenuation coefficient	Simulation for γ-ray from ^{60}Co source	Simulation for fission spectra gamma
Cake 1 4.554	0	234550	128205	1	1	1
	6.67	54689	23255	0.1814	0.1841	0.2418
	10	27430	9616	0.0750	0.0790	0.1250
	16.67	8150	1250	0.0098	0.0148	0.0357
	20	5335	284	0.0022	0.0064	0.0194
Multi-layer 6.126	0	234550	128205	1		
	6.67	43518	12828	0.1001		
	13.34	10143	832	0.0065		

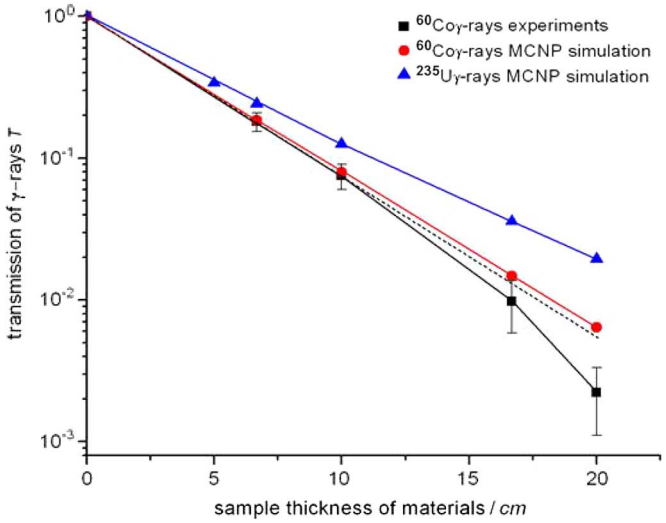

Fig. 9. Experiment & MCNP simulations for γ-rays attenuation of Cake1 samples.

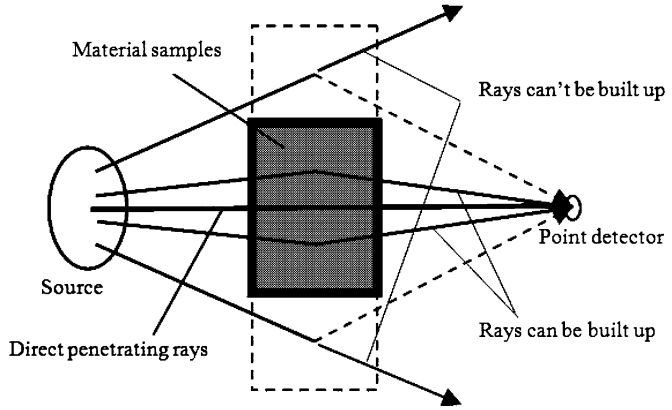

Fig. 10. Comparison of γ-rays dose enhancing effects between experiment and MCNP simulation. The sizes of material samples: dashed line pane-simulation; real line pane-experiment.

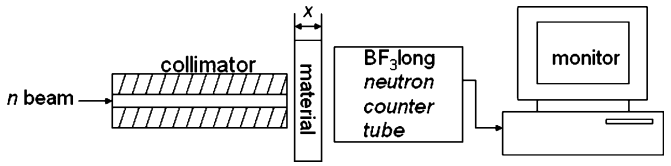

Fig. 11. The experimental setup diagram of neutron attenuation.

relationship. The revising method is that the counts increment of Compton scattering plain is accumulated into the net counts of full energy peak on γ-rays spectrum of ^{60}Co. In fact, an intuitionistic method to observe dose buildup effect is used by employing the NaI(Tl) crystal γ-rays spectrometer. However, the dashed line in Fig. 9 is still below the simulation data. This cannot be explained as simply γ-rays dose buildup effect as shown in Fig. 10. Other different conditions between experiment and simulation, such as the size and uniformity of source, source detector distance, source material distance, the position and size of collimator, and the detector size, can also produce the difference. The samples shielding performance to single energy γ-rays of ^{60}Co is better than γ-rays produced by thermal fission of ^{235}U, which is also shown in Fig. 9. In conclusion, the experimental results verified the correctness of optimal design method and reliability of the manufacture technology in γ-rays shielding.

B. Neutron Shielding Characteristics

Tandem electrostatic accelerator system and spontaneous fission neutron source of ^{252}Cf in China Institute of Atomic Energy (CIAE) were selected as neutron sources for neutron attenuation experiment. The Tandem electrostatic accelerator neutron source produces neutrons from the following nuclear reaction equations:

$$D + T \longrightarrow He + n(14.08\,\mathrm{MeV}) \tag{7}$$

$$D + D \longrightarrow {}^{3}He + n(2.45\,\mathrm{MeV}). \tag{8}$$

The neutron beam is exported by neutron collimator. The neutron attenuation experiment method and idea are the same as that of the gamma above. The experiment setup is shown in Fig. 11. All the results are shown in Fig. 12. At the top right corner in Fig. 12: (1) is Cake1 sample, (2) is multi-layers sample on service. Attenuation experiments for Cake1 samples were carried out at three neutron energy points of Tandem electrostatic accelerator: 0.479 MeV, 1.54 MeV, and 2.40 MeV and continuous energy spectrum of spontaneous fission neutron source of ^{252}Cf. The multi-layers samples were just carried out at 2.4 MeV. MCNP simulation for Cake1 to fission energy spectrum of ^{235}U neutron source was tested. The experimental data agree well with the simulation curve before neutron beam attenuated one thousandth at about 35 cm thickness. In particular, the Cake1 simulation of the transmission curve of neutrons produced by thermal fission of ^{235}U can fit with two

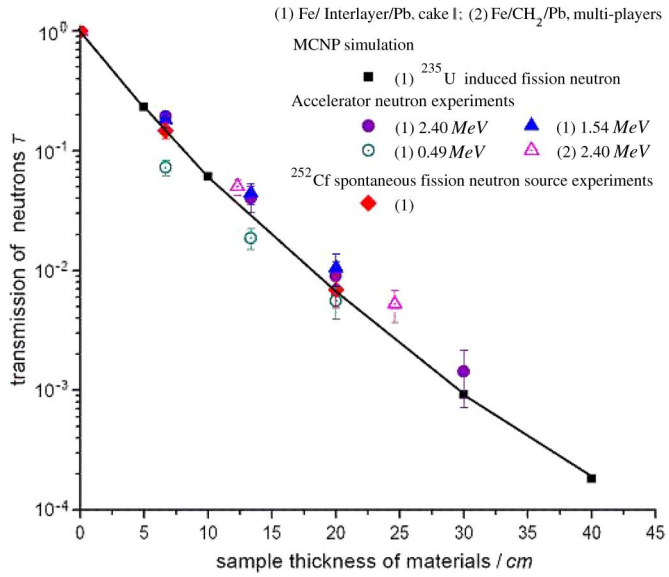

Fig. 12. Experimental test on neutron shielding performance of Cake1 and comparison to $\mathrm{Fe/CH_2/Pb}$ multi-layers.

experimental data of Cake1 samples irradiated by spontaneous fission neutrons of $^{252}\mathrm{Cf}$.

VI. Applications

The collimators in nuclear radiation measurement system were designed using the cakes to obtain favorable collimated beams requested by experimental physical scientists.

The trial production of the thick pinhole for fusion neutron penumbra imaging has been carried out according to the manufacturing process of shielding material.

VII. Discussion

In GA optimal design and shielding experiments, the selected material geometry model and experimental material samples were just slabs. If cylindrical and spherical geometry model and relative material samples were selected, actual shielding performance could be obtained. In other words, the shielding performance of the materials is better in applications than that in experiments because actual shields mostly have cylindrical or spherical geometry structure.

Due to lower intensities of radiation sources, the material samples are all too thin to test shielding effects perfectly in deep penetration situations in our experiments. The heat and radiation resistance of materials should be studied quantitatively in experiments. Therefore the related experiments should be carried out in the near future.

For the heavy metal powders, such as Fe, Pb and W, mixing with polymer, several precipitation phenomena appeared in the forming process when the mixture consists of high component of polymer, for example, more than 30%. In our study, the efforts to manufacture a new kind of special gradient material (SGM) by virtue of the precipitation phenomena are still under way. A permanent magnet is used to attract Fe powders from the polymer mixture, thus Pb and W powders remain precipitated in the mixture. Then the SGM with "middle heavy-light-heavy" density distribution could be produced. This kind of material is very suitable for the nuclear radiation shielding material.

Because Fe, Pb and W are separated completely to be independent parts of shield, the Cakes are the extreme product of the SGM. Furthermore, because Fe, Pb and W are ordinary materials, the production of Cakes could focus on just the Interlayer.

Fusion neutrons and γ-rays mixed radiation shielding material could be designed applying our GA optimal design method. It could design not only the shielding material component but also the thickness ratio of shield based on the interlayer products.

The tanks for nuclear fission waste and isotope transportation could be made adopting our interlayer forming technique partially.

VIII. Conclusions

The method to optimize in lightweight, compactness and high temperature sustaining for the neutrons and γ-rays mixed field shielding materials was established by genetic algorithms combined with the MCNP code. Several trial-manufacture samples were produced using the related manufacture technology. Shielding tests of samples verified that the correctness of optimal design method and reliability of the manufacturing process. The results of research can be wide applied to the practices of nuclear science and technology.

Acknowledgment

The authors would like to thank Zhiqiang Wang at the Metrology Department of the China Institute of Atomic Energy (CIAE), who provided accelerator and neutron dose monitoring. The authors also acknowledge valuable discussions with Professor Mingguang Zheng at the Shanghai Institute of Nuclear Power Engineering, and Professor Yuangang Duan at the Chengdu Nuclear Power Institute of China.

References

[1] A. N. Komarovskii, Design of Nuclear Plants USAEC Rep. AEC-tr-6722, 1965, pp. 1–34.

[2] W. Juapp, J. Taylor, C. Hudley, and N. Levoy, "Ducrete: A cost effective radiation shielding material," in *Proc. Starmet USA Spectrum Int. Conf. Nuclear and Hazardous Waste Management*, Chattanooga, TN, Sep. 24–28, 2000, pp. 336–342.

[3] R. C. Singleterry, Jr. and S. A. Thibeault, Materials for Low-Energy Neutron Radiation Shielding NASA/TP-2000-210281, Jun. 2000, pp. 1–14.

[4] T. S. Gates and J. A. Hinkley, Computational Materials: Modeling and Simulation of Nanostructured Materials and Systems NASA/TM-2003-212163, Mar. 2003, pp. 1–17.

[5] J. W. Wilson, F. A. Cucinotta, M. H. Kim, and W. Schimmerling, "Optimized shielding for space radiation protection," *Phys. Med.*, vol. 17 (Suppl. 1), pp. 67–71, 2001.

[6] National Council on Radiation Protection, Guidance on Radiation Received in Space Activities, NCRP Rep. No.98, Jul. 31, 1989, pp. 1–21.

[7] P. A. Lessing, Development of 'DUCRETE' INEL-94/0029, March 1995, pp. 1–16.

[8] "Recommendations of the international commission on radiological protection," Int. Commission Radiological Protection (ICRP), vol. 1, no. 3, Jan. 17, 1977, Publication 26.

[9] K. Okuno, "Neutron shielding material based on colemanite and epoxy resin," *Radiat. Protect. Dosim.*, vol. 115, no. 1–4, pp. 258–261, Dec. 2005.

[10] J. K. Shultis and R. E. Faw, "Radiation shielding technology," *Health Phys.*, vol. 88, no. 4, pp. 297–322, Apr. 2005.

[11] J. M. Brown, D. Curliss, and R. A. Vaia, "Thermoset-layered silicate nanocomposites. Quaternary ammonium montmorillonite with primary diamine cured epoxies," *Chem. Mater.*, vol. 12, no. 11, pp. 3376–3384, Oct. 2000.

[12] X. Kornmann, H. Lindberg, and L. A. Berglund, "Synthesis of epoxy-clay nanocomposites. Influence of the nature of the curing agent on structure," *Polymer*, vol. 42, no. 10, pp. 4493–4499, Feb. 2001.

[13] E. P. Giannelis, "Polymer-layered silicate nanocomposites: Synthesis, properties and applications," *Appl. Organometal. Chem.*, vol. 12, no. 10–11, pp. 675–680, Oct.–Nov. 1998.

[14] R. D. Albert and T. A. Welton, A Simplified Theory of Neutron Attenuation and Its Application to Reactor Shield Design, Westinghouse Electric Corp., Atomic Power Division, Pittsburgh, PA, WAPD-15, Nov. 1950.

[15] G. T. Chapman and C. L. Storrs, Effective Neutron Removal Cross Sections for Shielding, Oak Ridge National Laboratory, Oak Ridge, TN, ORNL-1843 (AECD-3978), Sep. 1955.

[16] A. W. Casper, Modified Fast Neutron Attenuation Functions, General Electric Corp., Atomic Products Div., Cincinnati, OH, XDC-60-2-76, Feb. 1960.

[17] Z. Michalewicz and C. Janikow, "GENOCOP: A genetic algorithm for numerical optimization problem with linear constrains," *Commun. ACM*, vol. 39, no. 12, Dec. 1996.

[18] J. F. Briesmeister, MCNP: A General Monte Carlo N-Particle Transport Code Los Alamos National Laboratory, NM, LANL Rep. LA-12625-M, Nov. 1993, Version 4A.

[19] A. H. Jaffey and J. L. Lerner, "Measurement of prompt neutron fission yield ($\overline{v_p}$) in thermal neutron fission of $^{232}\mathrm{U}$, $^{238}\mathrm{Pu}$, $^{241}\mathrm{Pu}$, $^{241}\mathrm{Am}$, $^{242}\mathrm{mAm}$, $^{243}\mathrm{Cm}$, $^{245}\mathrm{Cm}$ and in spontaneous fission of $^{244}\mathrm{Cm}$," *Nucl. Phys.*, vol. A145, no. 1, pp. 1–27, Apr. 1970.

[20] N. M. Schaeffer, Ed., Reactor Shielding for Nuclear Engineers, TID-25952, U.S. Atomic Energy Commission Office of Information Services, Jan. 1973.

[21] H. Hu *et al.*, "Optimized design of shielding materials for nuclear radiation," (in Chinese) *Atom. Ener. Sci. Technol.*, vol. 39, no. 4, pp. 363–366, Jul. 2005.

[22] Reactor Experiments, Inc., Catalog, Sunnyvale, CA.

[23] J. Lu and J. Chen, "High effective shielding material lead-baron polyethylene," (in Chinese) *Nucl. Power Eng.*, vol. 15, no. 4, pp. 370–374, Aug. 1994.

[24] K. Hattori, Y. Anayama, S. K. Hibanuma, K. Ueki, and S. Murakami, "Optimum arrangement for neutron shielding by KRAFTON series and SUS304," in *Proc. Topical Meeting Radiation Protection and Shielding-Advancements and Applications in Radiation Protection and Shielding*, Falmouth, MA, 1996, CD-ROM.

[25] A. Chapiro, *Radiation Chemistry of Polymeric Systems (High Polymers)*. New York: Wiley, Dec. 1962.

[26] C. L. Hanks and D. J. Hamman, Effect of Radiation on Electrical Insulating Materials Battelle Memorial Inst., Columbus, OH, Tech. Rep. N-69-33236; NASA-CR-101129; REIC-46, Jan. 1969, Radiation Effects Information Center.

[27] H. Shulman and W. S. Ginell, Nuclear and Space Radiation Effects on Materials-Space Vehicle Design Criteria, NASA-SP-8053, Jun. 1970.

[28] J. J. Licari and D. W. Swanson, *Adhesives Technology for Electronic Applications Materials, Processes, Reliability*. Norwich, NY: William Andrew, Jun. 2005, pp. 95–168.

[29] H. Schönbacher and M. Tavlet, "Radiation effects on structural materials for high-energy particle accelerators and detectors," in *Proc. Int. Workshop Advanced Materials for High Precision Detectors, Part IV, Materials and Environment*, Archamps, France, Sep. 1994, pp. 139–145.